Key Factors Influencing the Severity of Fluvial Flood Hazard from Tropical Cyclones

H. A. TITLEY,[a,b] H. L. CLOKE,[b,c,d] S. HARRIGAN,[e] F. PAPPENBERGER,[e] C. PRUDHOMME,[e,f,g] J. C. ROBBINS,[a] E. M. STEPHENS,[b,h] AND E. ZSÓTÉR[b,e]

[a] *Met Office, Exeter, United Kingdom*
[b] *University of Reading, Reading, Berkshire, United Kingdom*
[c] *Uppsala University, Uppsala, Sweden*
[d] *Centre for Natural Hazards and Disaster Science, Uppsala, Sweden*
[e] *ECMWF, Reading, Berkshire, United Kingdom*
[f] *University of Loughborough, Loughborough, United Kingdom*
[g] *U.K. Centre for Ecology and Hydrology, Wallingford, United Kingdom*
[h] *Red Cross Red Crescent Climate Centre, The Hague, Netherlands*

(Manuscript received 20 October 2020, in final form 12 March 2021)

ABSTRACT: Knowledge of the key drivers of the severity of river flooding from tropical cyclones (TCs) is vital for emergency preparedness and disaster risk reduction activities. This global study examines landfalling TCs in the decade from 2010 to 2019 to identify those characteristics that influence whether a storm has an increased flood hazard. The highest positive correlations are found between flood severity and the total precipitation associated with the TC. Significant negative correlations are found between flood severity and the translation speed of the TC, indicating that slower-moving storms that rain over an area for longer tend to have higher flood severity. Larger and more intense TCs increase the likelihood of having a larger area affected by severe flooding but not its duration or magnitude, and it is found that the fluvial flood hazard can be severe in all intensity categories of TC, including those of tropical storm strength. Catchment characteristics such as antecedent soil moisture and slope also play a role in modulating flood severity, and severe flooding is more likely in cases in which multiple drivers are present. The improved knowledge of the key drivers of fluvial flooding in TCs can help to inform research priorities to help with flood early warning, such as increasing the focus on translation speed in model evaluation and impact-based forecasting.

SIGNIFICANCE STATEMENT: Knowing ahead of landfall which TCs are likely to lead to significant river flooding will help those responsible for emergency planning make appropriate decisions to minimize loss of life and property. We compare 280 TCs and find that the cases with slow-moving, large, and intense cyclones, affecting areas with wet antecedent conditions, have the highest likelihood of experiencing widespread flooding. Slower-moving storms also have an increased risk of longer and more extreme floods. Our results show the importance of considering aspects such as the speed of forward movement along the whole flood early warning chain, from model evaluation and development, through to warning design and communication, to better inform forecast-based action prior to TC landfall.

KEYWORDS: Flood events; Hurricanes/typhoons; Precipitation; Tropical cyclones; Communications/decision making; Emergency preparedness; Emergency response

1. Introduction

Considering fluvial flood hazards in tropical cyclone (TC) forecasting and warning is important because this is a leading cause of mortality and damages (Rezapour and Baldock 2014). In the United States, drowning from excessive rainfall occurs in more TCs than deaths from any other cause (Rappaport 2014). Many of these fatalities occur outside of landfall counties (Czajkowski and Kennedy 2010) and in inland counties (Rappaport 2000). The U.S. residential losses from TC freshwater flooding are 2 times the losses from TC storm surge, with nearly half of these being in inland areas (Czajkowski et al. 2017). A multihazard approach considering both wind speed and rainfall has been shown to be more appropriate for risk-informed decision-making (Song et al. 2020), but studies investigating evacuation decision-making during hurricanes in the United States have shown that the key determining factor is the intensity of the storm on the Saffir–Simpson scale based on wind speed (Whitehead et al. 2000), with no significant relationship between the perceived risk of flooding and evacuation (Stein et al. 2010). Therefore, it is important to increase public awareness of the dangers of inland flooding, and provide a better understanding of those factors that influence the severity of flood hazard to those involved in emergency preparedness and disaster risk reduction activities.

Heavy rainfall can present a risk to communities regardless of the storm's intensity category. The U.S. National Hurricane Center (NHC) and the U.S. National Weather Service (NWS) both indicate the importance of other information beyond the storm's intensity-based category. The NHC states that "Rainfall amounts are not directly related to the strength of

Denotes content that is immediately available upon publication as open access.

Corresponding author: Helen Titley, helen.titley@metoffice.gov.uk

DOI: 10.1175/JHM-D-20-0250.1

TCs but rather to the speed and size of the storm, as well as the geography of the area'' (https://www.nhc.noaa.gov/prepare/hazards.php#rain). The NWS states that ''It is common to think the stronger the storm the greater the potential for flooding. However, this is not always the case. A weak, slow-moving tropical storm can cause more damage due to flooding than a more powerful fast-moving hurricane'' (https://www.weather.gov/jetstream/tc_hazards). The total rainfall from a TC in a given location is largely determined by the length of time a TC spends over that location, which is dependent on the size of the rainfall area and translational speed of the storm (Rogers et al. 2009). A slow along-track motion, or stalling near or after landfall, can lead to higher amounts of rainfall and a greater flood hazard, as seen during Hurricanes Harvey (2017) and Florence (2018). Larger TCs can also increase the rainfall hazard as they precipitate upon one spot for a longer time than smaller TCs moving at the same speed. They can also lead to more widespread flooding, leading to increased challenges for responders. Forecasting rainfall induced by TC landfall is determined by many factors, including the TC track, intensity, size and structure, as well as interaction with topography (Qiu et al. 2019), vertical wind shear (Chen et al. 2006), and other meteorological systems in the wider atmospheric environment. This can lead to seemingly similar landfall locations having different rainfall distributions (Cheung et al. 2018; Shi et al. 2017). Hydrological factors, such as soil conditions and orography, are also thought to have been important in determining which TC cases had elevated impacts from flooding (Rappaport 2000; Sturdevant-Rees et al. 2001).

While there is broad understanding, largely through case study or regional analysis (Saha et al. 2015; Hernández Ayala and Matyas 2016; Touma et al. 2019; Yu et al. 2017), of those factors influencing the rainfall related to TCs, systematic global analysis to objectively confirm these drivers and their relationships to downstream flood hazard is lacking. This study aims to address this gap and help provide more specific information in support of efforts to raise awareness of fluvial flood risk from TCs, by undertaking a systematic global analysis of the key meteorological and hydrological factors that lead to an increased fluvial flood hazard from TCs.

An improved understanding of the key factors that influence the severity of flood hazard from TCs is important to guide research work aiming to understand the predictability of fluvial flooding from TCs, to inform research priorities to improve the forecasts of flooding, and to guide planning and preparedness activities in the event of an advancing TC. Information on which TCs are likely to have storm surge and winds as their main hazard and which will also have substantial flood hazard is of vital importance for disaster risk reduction. While the strongest winds and largest storm surge usually occur near the center of intense TCs, rainfall and flooding often occur far from the center, spread far inland, and last beyond when the cyclone has weakened or dissipated (Villarini et al. 2014; Khouakhi et al. 2017). This has important consequences for evacuation, emergency management and recovery programs. If planners and responders better understand the likely severity of fluvial flooding for a given storm, and the locations likely to be at greatest risk from flooding, this can help with evacuation and emergency planning, response and recovery efforts.

This study develops three indices to represent the severity of fluvial flooding for TC cases in terms of the flood area, duration, and magnitude. These three flood severity indices are compared with TC and catchment characteristics in 280 landfalling TCs in the 10-yr period from 2010 to 2019 to identify the key factors that influence the severity of river flooding in TCs.

The remainder of this paper is set out as follows: section 2 details the data sources used in the study, and section 3 describes the methods used to select the TC cases, and calculate the TC characteristics, catchment characteristics and flood severity metrics for each case. Section 4 then compares the flood severity metrics for each storm with the TC and catchment characteristics to analyze the key factors that influence the severity of flood hazard from TCs. Section 5 discusses some important aspects of the results and where future work would be beneficial, and section 6 contains the main conclusions of the study.

2. Data sources

a. *IBTrACS*

The main observed TC track dataset used in this study is the International Best Track Archive for Climate Stewardship (IBTrACS) (Knapp et al. 2010, 2018). Where IBTrACS data are still listed as provisional (the 2018/19 and 2019/20 Southern Hemisphere seasons, and the 2019 season in the North Indian and North West Pacific basins), the track points are supplemented by the initial positions in the real-time advisories from each Regional Specialized Meteorological Centre (RSMC), which are collated at the Met Office for use in verifying TC track forecasts (Heming 2017; Titley et al. 2020).

The IBTrACS data are used to calculate the land footprint for each TC case (section 3a), over which to calculate the flood severity indices. The IBTrACS data also provide the TC intensity data [section 3b(1)], and are used to calculate the translation speed [section 3b(2)].

b. *Global Precipitation Measurement (GPM) IMERG*

Precipitation data are taken from the latest Integrated Multisatellite Retrievals for GPM (GPM IMERG Final Run V06) (Huffman et al. 2019). The ''Final Run'' data are used because they include gauge data where available to calibrate the rainfall satellite-derived observations and have been shown to capture TC precipitation patterns well, with closer agreement with gauge-based measurements than their predecessor for extreme events (Yuan et al. 2021). The data have a horizontal resolution of 0.1° and are extracted at a 30-min temporal resolution and then accumulated to give 24-h precipitation accumulation data. The precipitation summary metrics are described in section 3b(4).

c. *ERA5*

ERA5 is the European Centre for Medium-Range Weather Forecasts (ECMWF)'s latest comprehensive atmospheric reanalysis with a global horizontal grid resolution of approximately 31 km, or 0.281 25° (Hersbach et al. 2020). ERA5 mean

sea level pressure (MSLP) data were extracted from the Copernicus Climate Change Service (C3S) Climate Data Store (CDS) (Hersbach et al. 2018a) at 6-hourly intervals and used to calculate the size of the TC [section 3b(3)]. Daily ERA5 soil moisture content data were also extracted, along with soil type, for use in calculating the antecedent soil moisture saturation [section 3c(1)]. Precipitation accumulations were extracted hourly and summed to give 24-h precipitation totals to compare with GPM precipitation accumulations. Several studies have found large improvements in performance for precipitation in ERA5 relative to ERA-Interim (e.g., Beck et al. 2019; Tarek et al. 2020; Nogueira 2020), including for TC cases (Hersbach et al. 2018b). A recent study found that ERA5 agrees well with gridded gauge data in terms of the spatial distribution of typhoon precipitation, although it can underestimate the most extreme precipitation (Jiang et al. 2021).

d. *GloFAS-ERA5 reanalysis*

The severity of fluvial flooding from TCs is difficult to calculate in a consistent way from observations given the relative sparsity of river discharge observations, particularly in many areas impacted by TCs (Lavers et al. 2019). Therefore, this study uses the GloFAS-ERA5 global river discharge reanalysis (Harrigan et al. 2020b), as a proxy for river discharge observations. The Global Flood Awareness System (GloFAS) is designed to provide a global overview of upcoming flood events to decision-makers such as humanitarian organizations (e.g., Coughlan de Perez et al. 2016) as part of the Copernicus Emergency Management Service for floods. In GloFAS, ensemble meteorological forecasts from ECMWF are processed by the revised land surface hydrology scheme (HTESSEL) to create land surface runoff fields, with additional hydrological processes such as flow routing provided by the LISFLOOD hydrological model to forecast river discharge (Harrigan et al. 2020a; Alfieri et al. 2013; Balsamo et al. 2009, 2011; Van Der Knijff et al. 2010; Hirpa et al. 2018). Daily GloFAS-ERA5 river discharge reanalysis data, with a horizontal resolution of 0.1°, were extracted from the C3S CDS (Harrigan et al. 2019), for each day of 2010–19 and were used to define the flood severity in each landfalling TC case (section 3d).

Although GloFAS-ERA5 is partially dependent on model-derived precipitation and soil moisture, the groundwater and river routing parameters were calibrated against daily river discharge from 1287 observation stations worldwide (Hirpa et al. 2018) and a recent comprehensive global evaluation found it was skillful against a mean flow benchmark in 86% of catchments (Harrigan et al. 2020b). Other studies have compared GloFAS-ERA5 and observed discharge across regions (Ficchì and Stephens 2019; Towner et al. 2020), or in case studies e.g., Emerton et al. (2020), for Cyclones Idai and Kenneth in Mozambique. The use of GloFAS-ERA5 reanalysis data allows an analysis of the flooding across the whole area affected by each TC, rather than just at isolated points on the river network. It also allows a direct comparison of flood severity across all TC cases, using openly available data, in a way that would not be possible using discharge observations.

3. Methods

a. *Selecting TC cases and calculating their land footprint*

For the period 2010–19, the IBTrACS TC track data are filtered to only include those TCs with a landfall at tropical storm strength or above [≥34 kt (1 kt ≈ 0.51 m s^{-1})]. The 6-hourly latitude and longitude track position data are extracted where the storm is at or above tropical storm strength, and is over land or within 500 km of land. To decide the area, henceforth termed the "footprint," in which to calculate the flood severity for each TC, the following steps are taken (illustrated for Cyclone Eliakim, which impacted Madagascar in 2018, in Fig. 1):

1) The TC positions at the start and the end of each day are extracted and used to create a daily mask representing the area of precipitation defined as being associated with the TC, by calculating all grid points that lie within 500 km of that 24-h storm track segment. Most studies that have assigned a set radius for defining TC-related rainfall, have used a radius of either 500 km (Prat and Nelson 2013, 2016; Jiang et al. 2011; Luitel et al. 2018), 550 km (Zhou and Matyas 2017) or 5° (Guo et al. 2017).
2) The daily masks are combined to create an overall mask for the track of each TC.
3) The overall mask is combined with a land sea mask to create the final land footprint used to analyze the flood severity.
4) The number of valid 0.1° by 0.1° points (the GloFAS-ERA5 reanalysis resolution) in the land footprint is calculated, and the small number of TCs with fewer than 1000 points in their footprint (equating to an area of ~100 000 km^2) are excluded to ensure the footprints are large enough to allow a sensible comparison of the area affected by severe flooding.

This process results in 280 landfalling TC cases from 2010 to 2019 being included in the study (broken down by basin in Fig. 2). For each case, a set of TC characteristics, catchment characteristics, and flood severity measures are calculated to allow an analysis across the cases of the key factors influencing the severity of fluvial flooding.

b. *TC characteristics*

1) INTENSITY

The minimum MSLP and maximum sustained wind speed are extracted from IBTrACS at each track point, and the prelandfall value is used to identify the storm intensity for consideration in each case. To ensure that wind speed data are comparable between basins, 1-min maximum sustained winds are used where available.

2) TRANSLATION SPEED

Translation speed (speed in a forward motion) is calculated for each 6-h track segment by dividing the distance between the track points by 6 h. Three speed measures are then taken forward to consider in the analysis: (i) translation speed during the track segment where it makes landfall, (ii) average speed while the storm track is over land (the mean of the translation speeds

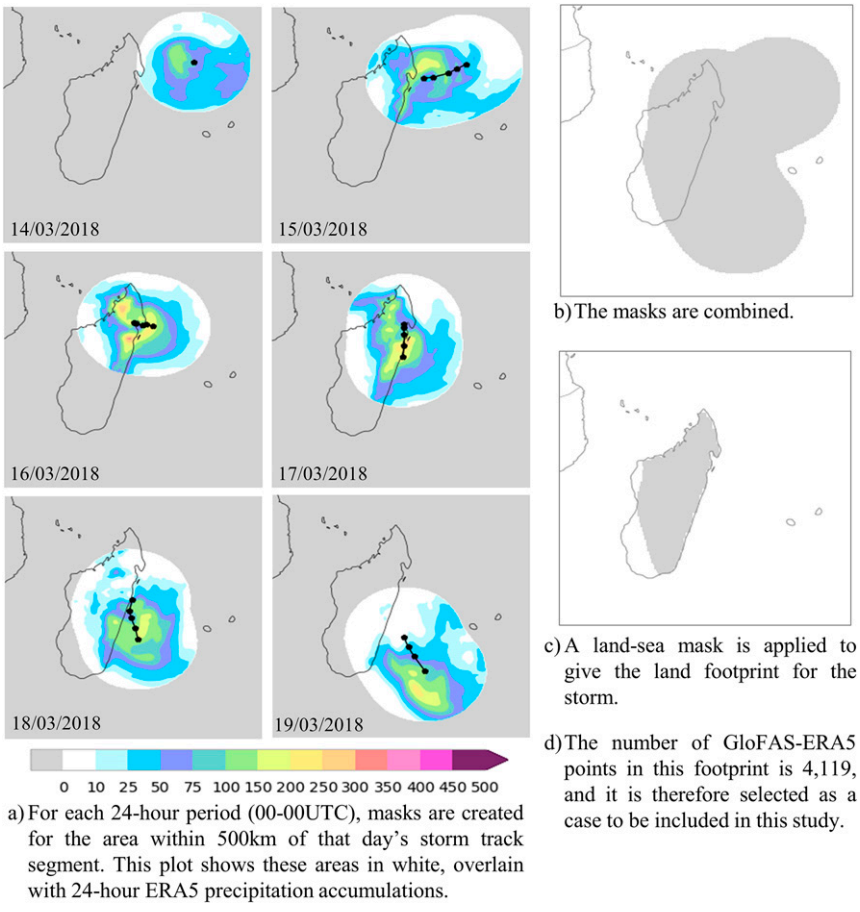

FIG. 1. Method for calculating the land footprint of each TC case, illustrated for Cyclone Eliakim, which impacted Madagascar in March 2018.

from all 6-hourly track segments over land), and (iii) minimum translation speed while the storm is over land (the minimum of the translation speeds from all 6-hourly track segments over land), to take account of storms that stagnate after landfall.

3) SIZE AND SHAPE

TCs span a huge range of sizes, with gale-force winds extending anywhere from ~20 km from the center to over 1000 km. A number of methods are commonly used to calculate storm size and shape, including the radial extent of winds reaching certain threshold values in knots (R43, R50, R64), the radius of the maximum winds (RMW), and the radius of the outermost closed isobar (ROCI) (Merrill 1984; Weber et al. 2014). The ROCI delimits the outermost extent of a TC's wind circulation and is the most relevant of these metrics for this study. Each RSMC will have its own, often subjective, procedures to calculate the ROCI recorded in IBTrACS, so to allow global comparisons this study recalculates the ROCI using ERA5 MSLP fields along the TC tracks. For each track point the MSLP field is centered on the storm location and then decomposed into tangential and radial coordinates, essentially unwrapping the field around the storm center. A search is carried out for the outermost closed MSLP isobar on each radial angle. The distance to this isobar is then averaged for all radial angles to give the overall ROCI, and is averaged for each quadrant (left front, right front, right rear, and left rear) to give shape information. Storm asymmetry is calculated by the ratio of the quadrant with the highest ROCI to that with the lowest ROCI. The average size and asymmetry in the day prior to landfall in each case are used in the subsequent analysis.

4) PRECIPITATION

The daily masks containing all points within 500 km of the storm track in each 24-h period (Fig. 1a) are applied to the 24-h precipitation accumulation data from GPM and ERA5, to obtain the precipitation considered to be associated with the TC. Three subsequent days are also included using the final mask to ensure that precipitation from any slow-moving remnants of the storm that may still contribute to flooding are included in the total storm precipitation. For the day prior to landfall, the proportion of the masked area with precipitation accumulations greater than 100 mm is calculated and included as a characteristic, to see how this information, which could be better estimated ahead of landfall, compares to flood severity.

To calculate the total storm precipitation, the masked daily precipitation fields are combined to give the overall storm-total

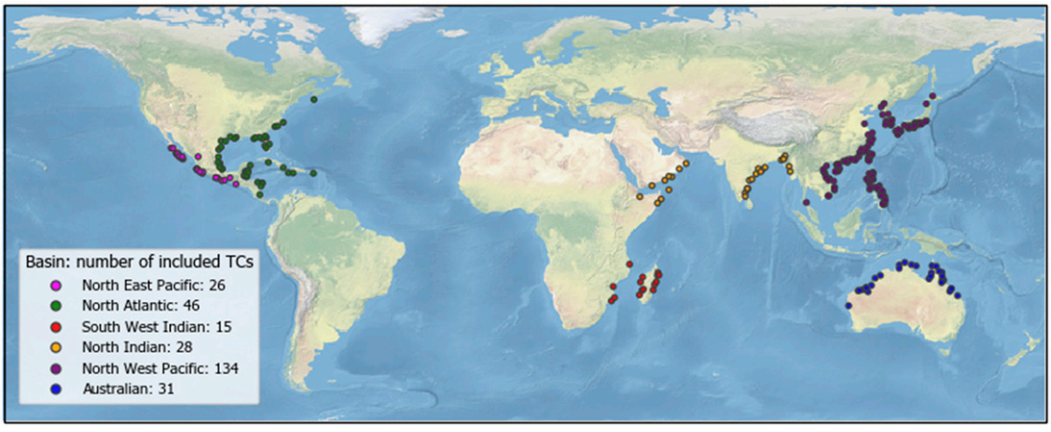

FIG. 2. The locations of the first land point in the track of the 280 TCs included in this study (2010–19), including the breakdown of cases by the TC basin. Note that no TCs are included in the South Pacific basin, where the only landfalls are in small island nations and therefore the land footprints were too small to allow for a fair comparison with the other cases.

GPM and ERA5 precipitation in the land footprint (illustrated for Cyclone Eliakim in Fig. 3). To investigate a range of precipitation characteristics in terms of their influence on the flood severity metrics, the following values are calculated from both GPM and ERA5:

1) the highest precipitation accumulation at any point in the land footprint area,
2) the average precipitation accumulation across the land footprint area,
3) the average precipitation accumulation for points in the land footprint area where the total is greater than 25 mm (giving an estimate of the average precipitation accumulated in those areas where the storm led to rainfall), and
4) the proportion of the land footprint area with precipitation accumulations greater than 25, 100, and 200 mm.

c. *Catchment characteristics*

1) ANTECEDENT SOIL MOISTURE SATURATION

ERA5-derived soil moisture saturation fields were calculated as a percentage of the progress along a scale from the permanent wilting point soil water content to the saturation soil water content [as specified by soil type in Table 8.9 of ECMWF (2020)]. The data were calculated on two levels: layer 1 (0–7 cm), and layers 1–3 combined (0–100 cm). For each TC case, the antecedent soil moisture saturation data were taken from the date prior to the storm coming within 500 km of land, to ensure the prestorm saturation levels were being recorded. The antecedent soil moisture saturation for the Cyclone Eliakim case is shown in Fig. 3c. For each layer, the average value in the storm land footprint was calculated, along with the proportion of the footprint with saturation greater than 90%.

2) OROGRAPHY AND GRADIENT

Two of the GloFAS input variables, detailing the orography and the gradient of each grid point, were extracted for each footprint area. The average orography and gradient within the storm footprint area were calculated for consideration in the data analysis.

d. *Calculating flood severity*

The period used to calculate the flood severity for each TC case was defined by setting the first date as the landfall date and the last date as a week after the final point in the cyclone track, to allow time for the affected watersheds to respond to the rainfall. For each day within this case period the GloFAS-ERA5 discharge data in the land footprint area were compared with return period flood thresholds to calculate the return period exceeded at each point. The return period thresholds were taken directly from GloFAS, where they are determined from the GloFAS-ERA5 river discharge reanalysis, by fitting a Gumbel extreme value distribution on the annual maxima time series over the 1979–2018 period (Alfieri et al. 2019; Harrigan et al. 2020a; Zsótér et al. 2020).

Flood severity can be defined in several ways, each measuring a contrasting property of the flood hazard that may be of particular relevance to different stakeholders. In this study the flood severity is calculated in the following three ways for each storm:

1) *Flood severity (area)*: This is defined as the percentage of GloFAS grid points within the storm's footprint where the discharge exceeds the 5-yr return period value for that point at any date during the case period. This has been termed "area" to simplify the decomposition of flood severity into three component parts, but it is more akin to "floodiness" (Stephens et al. 2015) defined over a storm's footprint than it is to measures of inundation extent. For Cyclone Eliakim, the flood severity (area) was 22% (Fig. 3d).
2) *Flood severity (duration)*: This is defined by selecting those points where the 5-yr return period was exceeded on at least one day, and then calculating the average number of days for which the 5-yr return period was exceeded at those points. This value is set to zero for

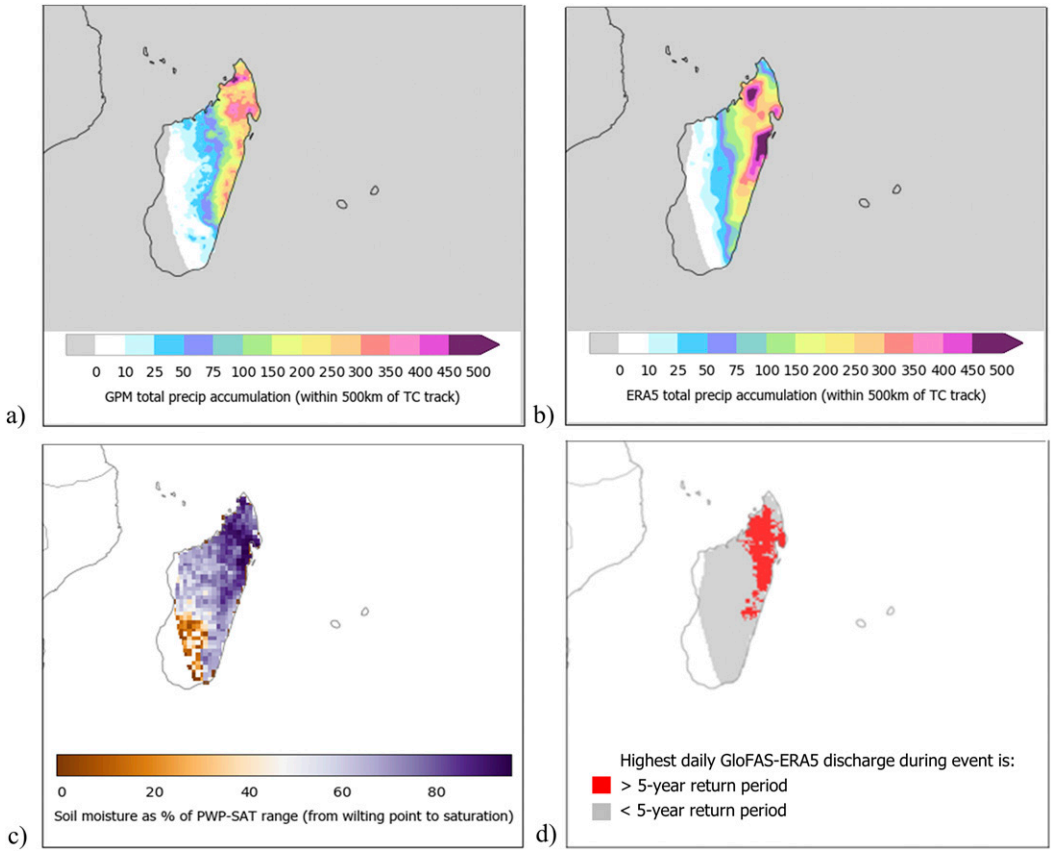

FIG. 3. Cyclone Eliakim (2018): (a) total event precipitation calculated from GPM, (b) total event precipitation calculated from ERA5, (c) antecedent soil moisture saturation in the top layer of soil, and (d) GloFAS-ERA5 points that exceeded the 5-yr return period during the event (22% of land footprint).

cases in which no points exceed the threshold at all during the case period.

3) *Flood severity (magnitude)*: For this magnitude-based definition the data are filtered to only include points that have an upstream area of greater than 1000 km^2, to focus on the magnitude of the flooding on larger rivers in the footprint. The magnitude of the flood is defined by first calculating the maximum return period that is exceeded at each of these river points during this TC event, and then ranking the points from highest to lowest and calculating the average return period exceeded over the top 100 points. The return periods are capped at 200 years as a sensible upper limit, given that the return period thresholds are generated on a 40-yr sample (Harrigan et al. 2020a). In this way the magnitude-based definition of flood severity compares the most severely affected river points in each TC case, in terms of the extremeness of the discharge levels experienced.

4. Results

a. Comparison of flood severity measures

The flood severity of all the TC cases, split geographically by the TC basin, is summarized in Fig. 4. For all basins other than the South Indian Ocean, most of the cases have relatively low flood severity (area) (median of 1%–5%), but each basin has several cases with higher flood severity. However, in the South Indian Ocean basin, more of the cases have a higher flood severity (area), with the median of 13% (Fig. 4a) found by a Kruskal–Wall H test to be significantly different from the other basins (significance level $p < 0.01$). For flood severity (duration) the median duration for those points exceeding the 5-yr return period threshold is between one and three days in all regions (Fig. 4b). The median duration was higher for the Australian basin and the lower for the North West Pacific (both significant at $p < 0.01$). For flood severity (magnitude) the South Indian Ocean is again shown to have a higher median value than other regions have (significant at $p < 0.01$). All basins have some cases in which very high return periods are exceeded (Fig. 4c).

There are significant positive Spearman correlations between the three flood severity measures (Fig. 5). Although the correlations are strong (>0.5 in each case), there are some cases in which storms have a very high flood severity in one measure and not in another. Good examples of this are Typhoon Hagibis (2019) and Typhoon Lan (2017), which can be seen in the bottom right of the plot in Fig. 5a, with highest flood

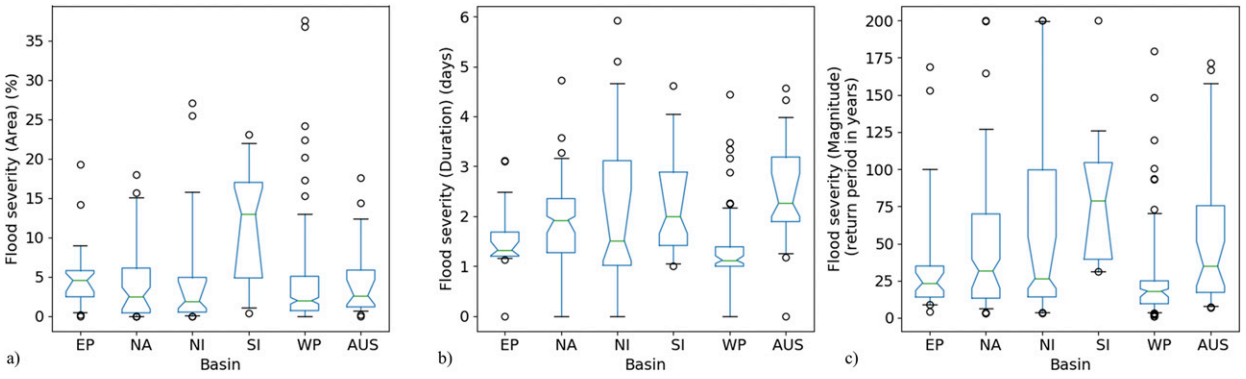

FIG. 4. Box-and-whisker plot showing (a) flood severity (area), (b) flood severity (duration), and flood severity (magnitude) grouped by TC basin [Australian (AUS), eastern Pacific (EP), North Atlantic (NA), ''North Indian'' (NI), ''South Indian'' (SI), and ''North West Pacific'' (WP)]. In all of the box-and-whisker plots in this study, the box extends from the Q1 to Q3 quartile values of the data and the whiskers extend from the 5th to the 95th percentiles. Outliers beyond this point are plotted as circles. The median is shown by a green line, with the 95% confidence bounds in that median shown by the notched area of the box, calculated by bootstrapping.

severity (area), but where most of that flooding was very short lived, with flood severity (duration) of only around 1 day. This emphasizes the importance of considering multiple indices, to take into consideration all characteristics of the flood severity.

The top 10 most severe cases according to each of the flood severity indices are shown in Table 1. All basins have storms represented in the lists. Many storms appear in the top 10 for two of the indices, and two storms, Cyclone Luban (2018) and Cyclone Idai (2019) appear in all three lists. Table 2 contains a summary of the impacts from the TC cases that appear in at least two of the three top-10 lists. While it is harder to ascertain whether there were cases with severe impacts that were not highlighted, the fact that all of the storms in Table 2 had significant impacts from flooding indicates that the methods used in this paper have correctly highlighted high-impact cases of fluvial flooding from TCs.

b. Relationships between flood severity and case characteristics

1) CORRELATIONS

The Spearman's rank correlation coefficients between the flood severity metrics and all the calculated storm and catchment characteristics are shown in Fig. 6. A comparison between GPM and ERA5 rainfall (not shown) revealed very strong correlations, so only the ERA5 precipitation variables are included. All the flood severity variables are significantly correlated with each other, as was seen in Fig. 5. All precipitation variables (both for the precipitation field prior to landfall and for the accumulated precipitation variables within the footprint) are significantly positively correlated with the flood severity (area) index, with the highest correlations for the average accumulation in the footprint where it rained (0.58) and for the percentage of the footprint over 100-/200-mm

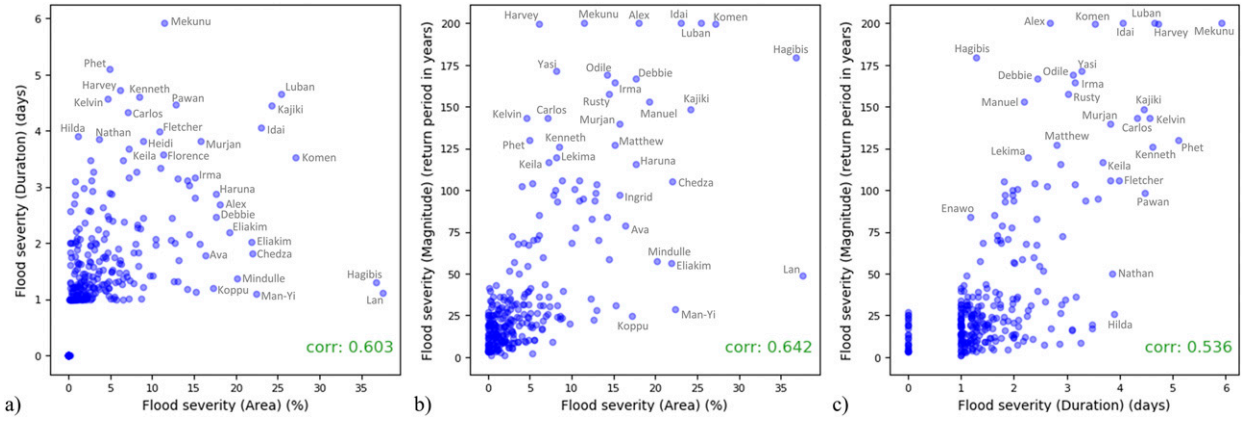

FIG. 5. Scatterplots of the different flood severity indices: (a) flood severity (area) vs flood severity (duration); (b) flood severity (area) vs flood severity (magnitude); and (c) flood severity (duration) vs flood severity (magnitude). The Spearman's rank correlation coefficient is displayed on each plot. Points are annotated with the storm name if they have high values on either axis or are outliers to the general pattern.

TABLE 1. The 10 highest-ranked TCs for each flood severity measure (in boldface type if that TC case is in the top 10 for two of the three indices, and in boldface italic if it is in the top 10 of all three indices). The regions are defined in the caption of Fig. 4.

Rank	Flood severity (area)	Flood severity (duration)	Flood severity (magnitude)
1	Lan (WP; 2017)	**Mekunu** (NI; 2018)	Alex (NA; 2010)
2	**Hagibis** (WP; 2019)	Phet (NI; 2010)	***Luban*** (NI; 2018)
3	**Komen** (NI; 2015)	**Harvey** (NA; 2017)	**Mekunu** (NI; 2018)
4	***Luban*** (NI; 2018)	***Luban*** (NI; 2018)	***Idai*** (SI; 2019)
5	**Kajiki** (WP; 2019)	Kenneth (SI; 2019)	**Harvey** (NA; 2017)
6	***Idai*** (SI; 2019)	Kelvin (AUS; 2018)	**Komen** (NI; 2015)
7	Man-Yi (WP; 2013)	Pawan (NI; 2019)	**Hagibis** (WP; 2019)
8	Chedza (SI; 2015)	**Kajiki** (WP; 2019)	Yasi (AUS; 2011)
9	Eliakim (SI; 2018)	Carlos (AUS; 2011)	Odile (EP; 2014)
10	Mindulle (WP; 2016)	***Idai*** (SI; 2019)	Debbie (AUS; 2017)

accumulations (0.57/0.54). For flood severity (duration), there is no significant correlation with the precipitation prior to landfall, but there are significant correlations with most total storm accumulation measures. For flood severity (magnitude), there are positive correlations with all precipitation variables apart from the percentage of the footprint over the lowest value of 25 mm.

The storm *intensity* variables, MSLP and wind speed at landfall, are significantly negatively (−0.18) and positively (0.13) correlated with flood severity (area), respectively. This shows that generally the more intense the storm (lower MSLP minima and stronger winds), the greater the flood severity. However, neither intensity variable is significantly correlated for flood severity (duration) or flood severity (magnitude), so it is not always the case that a strong storm will lead to severe flooding in terms of duration or magnitude, or that a weaker storm cannot cause significant flood events. A comparison of the distribution of flood severity values for TC cases split into those that are tropical storms at landfall with those that have equivalent hurricane or major hurricane strength (Fig. 7) confirms that all storm categories have some cases with both low and high flood severities. There are no significant differences between the severity of flooding in tropical storms and hurricanes, but for major hurricanes there is a notable increase in the upper quartile range and the median is significantly higher for the area and magnitude definitions of flood severity (Kruskal–Wall H test with $p < 0.01$).

The three *translation speed* variables are all significantly negatively correlated with all the flood severity indices i.e., slower-moving storms tending to have greater flood severity when considered in terms of area, duration and magnitude. The strongest correlations are with the duration of flooding (−0.31, −0.32, and −0.33, respectively, for the translation speed at landfall, the average translation speed over land, and the minimum translation speed over land).

The *storm size* as measured by the ROCI is significantly positively correlated with flood severity (area) (0.12), indicating that larger storms tend to have a greater percentage of the land footprint exceeding the 5-yr return period. There is no significant correlation with flood severity (duration) or flood severity (magnitude), and no significant correlation of *storm asymmetry* with any of flood severity measures.

The relationship between flood severity and *soil saturation* is complex and varies with each of the flood severity indices. For

TABLE 2. A summary of the impacts from those TCs that appear in the top 10 for at least two of the flood severity measures (in boldface type if that TC case is in the top 10 for two of the three indices, and in boldface italic if it is in the top 10 of all three indices). All are TCs that led to significant impacts.

Case	Summary of impacts
Idai (SI; 2019)	Severe flooding in Mozambique, Malawi, and Zimbabwe, leading to a major humanitarian crisis; damages of at least $2.2 billion (2019 USD), 1.85 million people in need of humanitarian assistance, and over 600 fatalities in Mozambique alone (Emerton et al. 2020); deadliest TC recorded in the South West Indian Ocean basin
Luban (NI; 2018)	Flooding in Somalia, Oman, and Yemen, with 14 deaths in Yemen, with damages in the country estimated at U.S. $1 billion (Associated Press 2018)
Hagibis (WP; 2019)	98 confirmed deaths in Japan and more than 270 000 households left without power across the country; severe damage to transport infrastructures
Komen (NI; 2015)	Komen led to 45 deaths in Bangladesh, 83 in India, and 39 deaths in Myanmar
Kajiki (WP; 2019)	At least 6 fatalities in Vietnam, with agricultural losses estimated at U.S. $12.9 million
Mekunu (NI; 2018)	31 fatalities (Socotra island, Yemen, and Oman); severe flooding led to power outages, and landslides
Harvey (NA; 2017)	Unprecedented flooding in Texas inundating hundreds of thousands of homes, displacing more than 30 000 people, and prompting more than 17 000 rescues; over 100 fatalities

FIG. 6. Spearman's rank correlation coefficients of the flood severity variables with the TC characteristics and catchment characteristics for each TC case. Those with a Spearman's rank correlation coefficient with a significance value <0.05 are marked in boldface type with an asterisk.

flood severity (area), all the soil saturation metrics have positive correlations, showing that cases with more saturated antecedent soil conditions tend to have greater flood severity. However, a different pattern is shown for the other two flood severity indices (duration and magnitude), where there are significant negative correlations with the average soil moisture saturation in the top 100-cm layer (-0.27 and -0.15, respectively).

There is a significant positive relationship of average *orography* and flood severity (area) (0.24), and there are significant

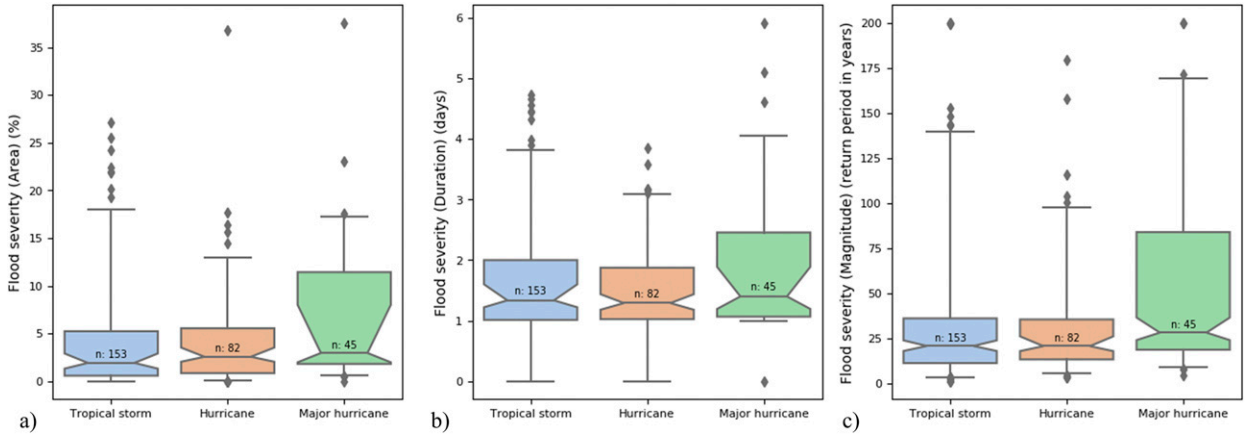

FIG. 7. Flood severity [(a) area, (b) duration, and (c) magnitude], for three categories of TC calculated based on the maximum wind speed at landfall taken from IBTrACS: (i) tropical storm (34–63 kt), (ii) equivalent hurricane strength (64–95 kt), (iii) equivalent major hurricane strength (96+ kt). In actuality, different storm categories and thresholds are used by different RSMCs when defining intensity, but to compare across basins the categories from the Saffir–Simpson scale are used here. The 95% confidence bounds in the median is shown by the notched area of the box, calculated by bootstrapping. The number of cases in each category is overlain.

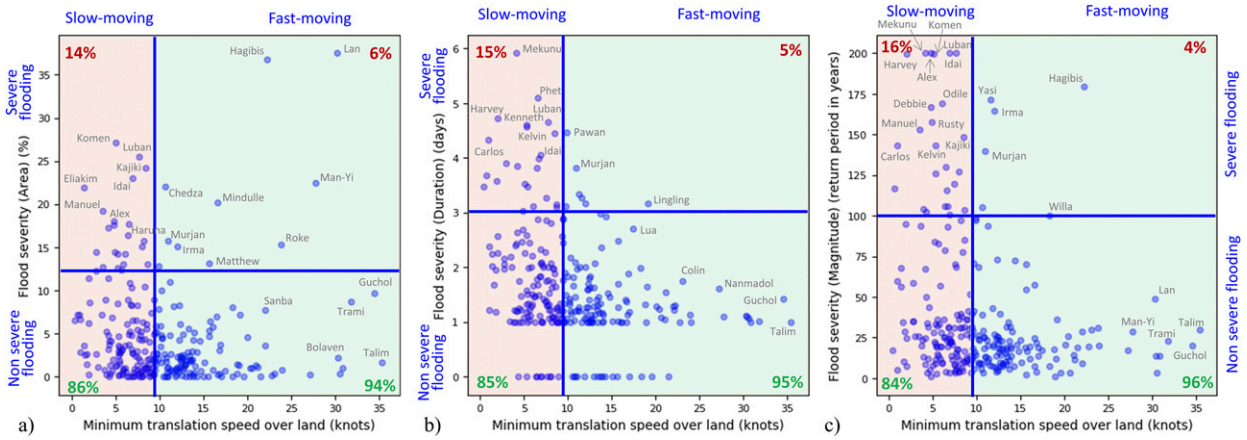

FIG. 8. Illustration of the conditional probability technique for examining the relationship between minimum translation speed over land and flood severity. The blue lines divide the plot into quadrants based on the median translation speed (9.19 kt) and the 90th percentile of the flood indices [12.86% for flood severity (area), 3.10 days for flood severity (duration), and 102.59 for flood severity (magnitude)]. There are, therefore, equal numbers of cases in the orange and green halves of the plots, and the upper section of the plot displays the 10% of the TC cases with the most severe flooding. The numbers in the top-right and top-left quadrants can be compared to see if there is an elevated risk of severe flooding for slow-moving storms. Points are annotated with the storm name if they have high values on either axis or are outliers to the general pattern. The Spearman's rank correlation coefficients for each plot are (a) −0.22, (b) −0.33, and (c) −0.26.

negative correlations of the average *gradient* with flood severity (duration) (−0.44) and flood severity (magnitude) (−0.31), so lower gradients would tend to have greater flood severity in terms of the flood duration and magnitude.

2) CONDITIONAL PROBABILITIES

Conventional wisdom is that translation speed is a significant risk factor leading to increased flood severity. Significant relationships were shown between the flood severity indices and the translation speed of the TC in Fig. 6, but the correlations are perhaps lower than anticipated, at −0.22, −0.33, and −0.26 for the minimum translation speed over land when compared with flood severity as measured by area, duration, and magnitude, respectively. However, if we look in more detail at scatterplots for these relationships, and apply a conditional probability technique to split the plot into four quadrants, further useful information can be found (Fig. 8). The *x* axis is split by the median value of the minimum translation speed over land, to designate slow-moving and fast-moving storms. A sensitivity analysis (not shown) was used to select which percentile of the *y* axes (the flood severity scores) to use to designate nonsevere and severe flooding cases. The 90th percentile was selected as the threshold that gave the best combination of having sufficient cases included in the upper section while also focusing in on the more severe cases (the top 10%). The conditional probability of having severe flooding if the storm is slow moving is then calculated. For flood severity (area), the conditional probability of having severe flooding if the storm is slow moving is 14%, more than double the conditional probability if the storm is fast moving (6%) (Fig. 8a). So although there are a few cases (e.g., Hagibis, Man-Yi, and Lan) in the upper-right quadrant of Fig. 8a in which flood severity is high in fast-moving storms and there are many cases in which slow-moving storms do not lead to severe flooding, overall there is a greater risk of severe flooding in slow-moving storms, with a significant cluster of storms with high flood severities and low translation speeds (e.g., Komen, Idai, Luban, Kajiki, and Eliakim). The results when we apply the same conditional probability technique to the other two flood severity metrics are even clearer, with 3 times the probability of having a severe flooding event for slow-moving storms for flood severity (duration), and 4 times the probability of a severe flooding event for slow-moving storms for flood severity (magnitude) (Figs. 8b,c).

Fast movement of TCs appears to often mitigate severe flooding, and slow movement increases the likelihood of severe flooding, but these patterns are not seen in all cases. The role of other factors in moderating this relationship can be examined by comparing conditional probability plots of flood severity with several different characteristics, selected based on the correlation results shown in Fig. 6 (Fig. 9). Flood severity (area) is used to examine in more detail the interplay between characteristics, as the extent of the severe flooding across the whole area affected by the TC is perhaps the most relevant when considering preparedness and recovery activities such as evacuation planning. The strong relationship between flood severity and the percentage of the footprint with high precipitation totals can be seen in Fig. 9a, with only 2% of the cases lower than the median precipitation having severe flooding. When the conditional probability technique is applied to the average soil saturation in the top layer of the soil, there is found to be more than double the risk (14% as compared with 6%) of having severe flooding where there is high soil saturation (Fig. 9b). Figures 9c–e show three of the TC characteristics that may play a role in increasing the overall precipitation accumulation: intensity, translation speed, and size. For the more

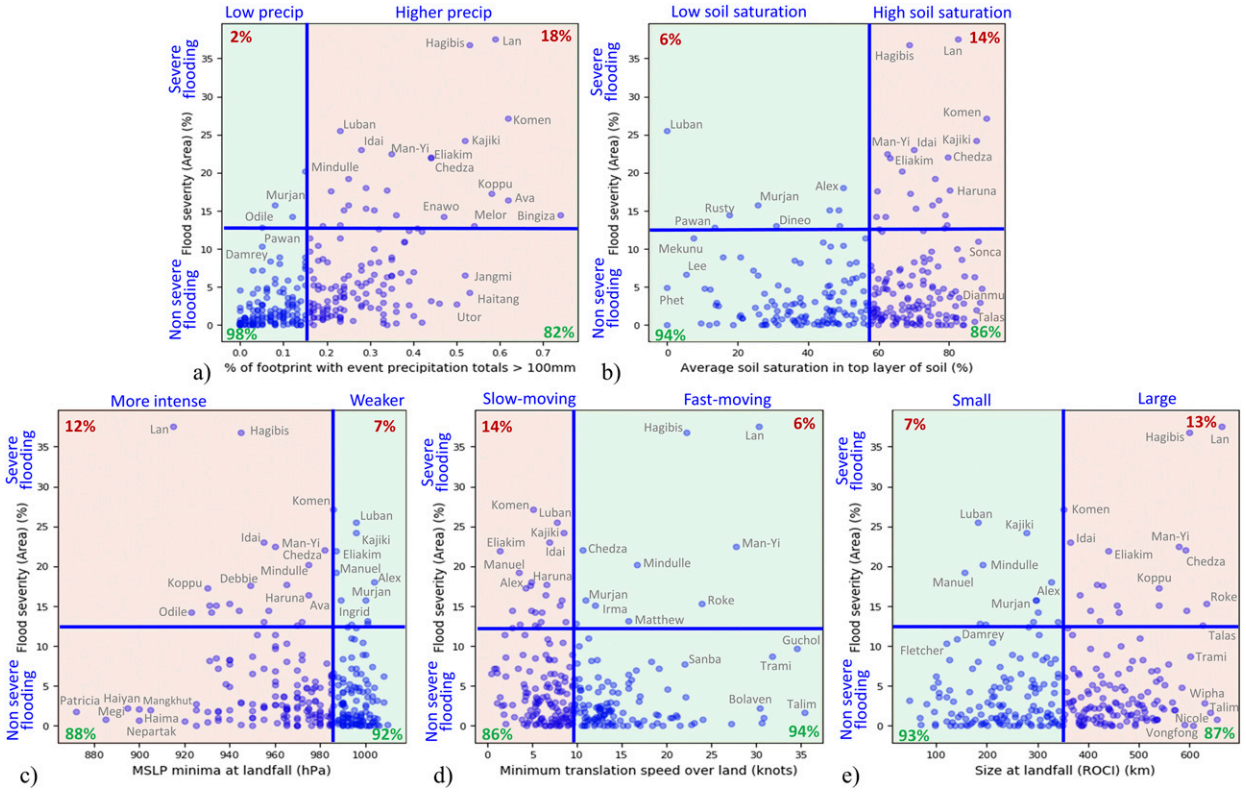

FIG. 9. Scatterplots for the flood severity (area) indices against (a) the percentage of the footprint with event precipitation totals greater than 100 mm, (b) average soil saturation in the top layer of soil, (c) mean sea level pressure minima at landfall, (d) minimum translation speed over land, and (e) size at landfall (ROCI). Each plot has the conditional probability technique applied using the median of the variable and the 90th percentile of the flood severity to create the quadrants. The Spearman's rank correlation coefficients for each plot are 0.57 for (a), 0.15 for (b), −0.18 for (c), −0.22 for (d), and 0.12 for (e).

intense storms, there is a small increased probability of severe flooding (12%) when compared with the less intense storms (7%) (Fig. 9c). The doubling of the likelihood of severe flooding for slow translations speeds, as shown in Fig. 8a, are repeated in Fig. 9d, while Fig. 9e shows the conditional probability results for TC size, with nearly double the risk of severe flooding for large storms (13%) relative to small storms (7%).

Typhoons Man-Yi (2013), Hagibis (2019) and Lan (2017) appear as relative outliers in the upper right quadrant of Fig. 9d (fast-moving storms where flood severities were unexpectedly high or very high). On Fig. 9e it can be seen that these are all very large storms, indicating that the size of these storms may have been a significant factor contributing to their high flood severity, acting to override the mitigative nature of their fast translation speed. They are also categorized in the more intense category for intensity (Fig. 9c), and the high soil saturation category (Fig. 9b). Thus, in these cases the high translation speed of these typhoons did not prevent a severe flood event due to the presence of several other risk factors.

A similar conditional probability analysis for the other two flood severity measures (duration and magnitude) (not shown) found that the main driving factor from the TC characteristics was the translation speed of the storm. The other main risk factors were from the catchment characteristics, with drier soils and lower gradients being associated with a large increase in the risk of having a longer and higher magnitude flood event. These results show that the influence of the catchment characteristics on the duration and magnitude of flooding is greater than for the flooding measured in terms of the area.

3) INTERPLAY OF CHARACTERISTICS

To investigate further how the combination of several factors helps to determine the overall flood severity, two characteristics, TC translation speed and TC size, have been used to split the cases into four categories based on whether they are larger or smaller than the median size and faster or slower than the median translation speed (Fig. 10). For flood severity (area), cases in which the TC is both slow and large have the highest median and upper quartile range, followed by slow and small, then fast and large, and finally fast and small cases. Meanwhile for flood severity (duration) and flood severity (magnitude) there is a clearer split between the fast types and the slow types, showing that for flood duration and magnitude the translation speed of the storm is a more important factor than the size of the storm.

This process is taken further by grouping each TC case depending on how many of the four risk factors found in Fig. 9

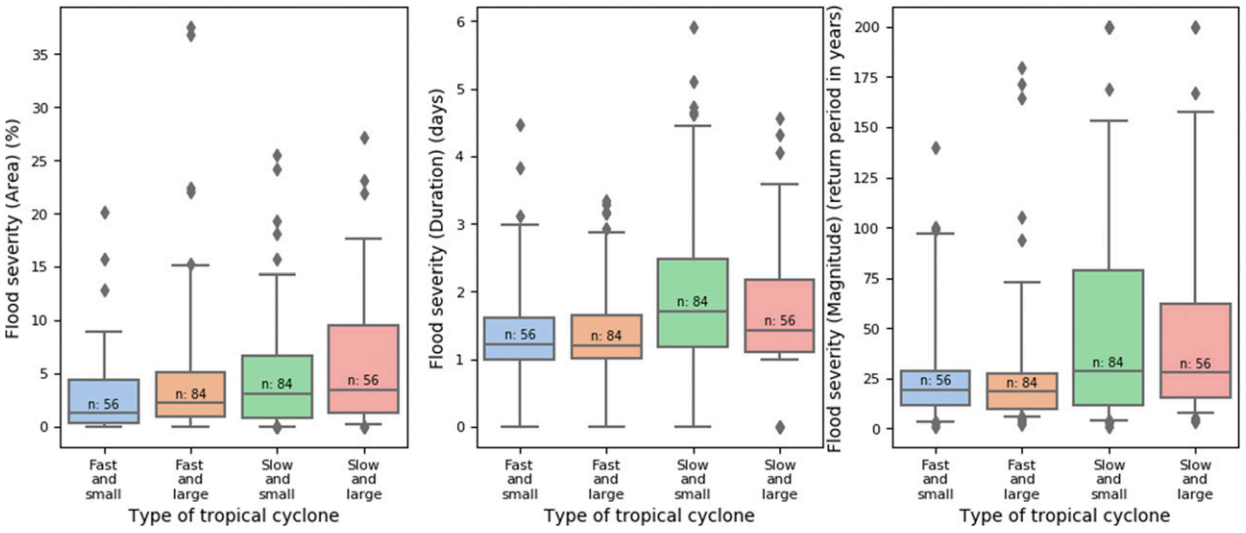

FIG. 10. Flood severity [(left) area, (center) duration, and (right) magnitude] for four categories of TC: (i) fast and small, (ii) fast and large, (iii) slow and small, and (iv) slow and large. The number of cases in each category is overlain.

(slow-moving storm, large storm, intense storm and wet antecedent conditions) are present (Fig. 11). Total precipitation is not included here as we are focusing on the factors that influence that precipitation, that are easier to estimate a priori when assessing the risk associated with a storm in forecast mode. Figure 11a shows that the likelihood of a higher flood severity increases the more risk factors are present. Figure 11b splits the categories by which of the risk factors are present. The storms that are classed as having all four risk factors (slow, large, strong, and wet) have the highest median flood severity and the highest upper quartile range. Within those cases that have three risk factors, cyclones that are slow and large with wet antecedent conditions stand out as having a high upper quartile range. For those cases with two risk factors, the highest median value is for cases with slow TCs with wet antecedent conditions, while where only one risk factor is present, there are higher flood severities for slow storms.

5. Discussion of the key outcomes

a. *Applying flood severity metrics to TC footprints*

This study has implemented three flood severity indices designed to measure the severity of flooding in TCs, based on (i) the area affected; (ii) the duration of the flooding; and (iii) the magnitude of the flooding in the most severely affected areas. Although the different flood severity measures are all significantly positively correlated with each other, there are cases in which a storm has a very high flood severity in one measure and not in another, for example, where a large area is affected but flood duration is low. Some of the drivers of an enhanced flood severity found in this study are consistent whether considering the area affected, duration, or magnitude e.g., high total precipitation and low translation speed, whereas some drivers are only significant for one or two of the indices e.g., large storms and the area-based index, and gentler slopes with the duration- and magnitude-based indices. This emphasizes the importance of considering multiple indices to take into consideration all characteristics of the flood hazard, especially given that stakeholders may have differing priorities. An organization with responsibility for emergency planning across a large geographical area would be particularly concerned about the extent of the area being affected by flooding, whereas an individual in an area prone to flooding may be most concerned about the magnitude of flooding likely to be experienced.

b. *Importance of precipitation and translation speed*

The strongest relationships are found with the metrics summarizing the event total precipitation, showing the importance of increasing the availability and profile of precipitation forecasts in TC forecast communication and verifying the ability of models that drive flood forecasting systems to forecast the precipitation associated with TCs.

Of the other TC characteristics, the speed of forward movement of the TC is found to be a key factor influencing the severity of the fluvial flood hazard, in terms of its area, duration and magnitude. This confirms that slower-moving storms, which rain over a given area for longer, tend to have higher flood severity, and that greater focus should be given to translation speed in forecast warnings and communication. Climate change is thought to have caused a general weakening of summertime tropical circulation, decreasing the translation speed of TCs (Kossin 2018). This, combined with an expected increase in the magnitude of rainfall rates in TCs (Knutson et al. 2010), is likely to lead to an increased fluvial flood hazard from these events in the future.

c. *Presence of flood hazard at all levels of storm intensity*

TC intensity is positively correlated with the flood severity as defined by area, but not significantly correlated with the duration or magnitude of the flooding. A further analysis splitting cases into those of equivalent tropical storm, hurricane, and

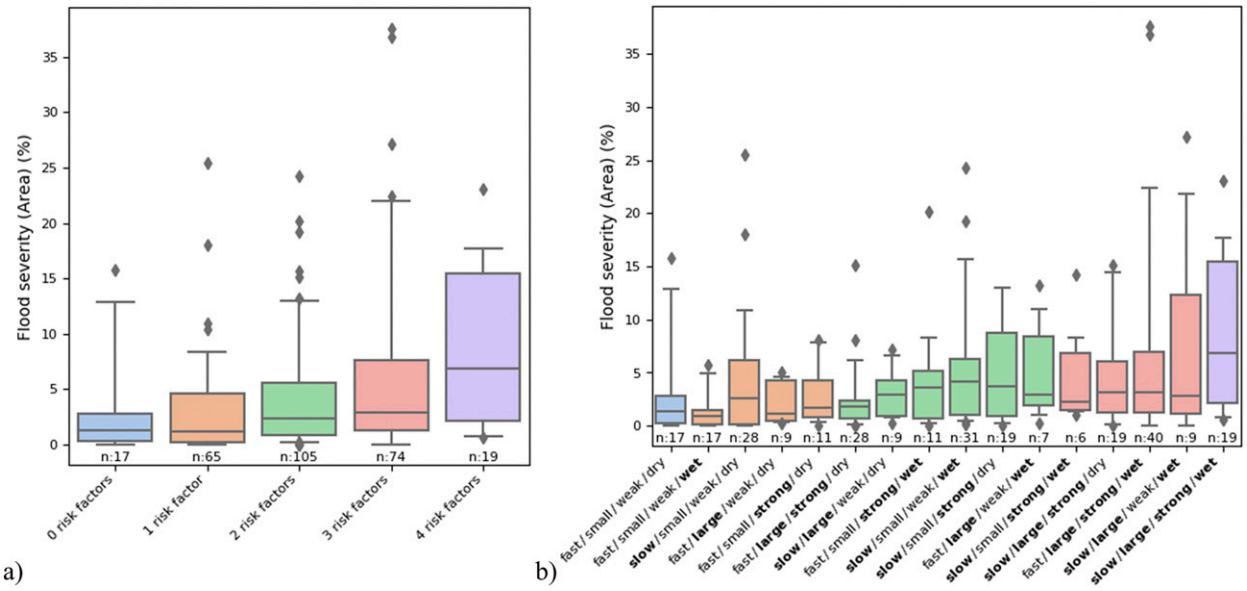

FIG. 11. Flood severity (area), for TCs grouped by risk factors (slow-moving storm, large storm, intense storm, and wet antecedent conditions) (a) grouped according to how many of the risk factors they possess and (b) further split by which risk factors (highlighted in boldface type) are present in each group. The number of cases in each category is displayed below the box plot.

major hurricane strength, showed that all three have cases spanning the full range of flood severity values. This shows the importance of forecasting agencies continuing to emphasize to both the public and to organizations involved with disaster risk reduction preparedness and response activities that the fluvial flood hazard can be severe in all categories of TC.

d. Complex relationship between flood severity and antecedent soil moisture

Conventional wisdom, established by looking at small to medium sized flood events, is that higher levels of soil moisture saturation would lead to an increased risk of flooding (Berghuijs et al. 2019). However, when dealing with the extreme precipitation totals that can be found in TC events, the relationship appears more complex. For flood severity (area), there are indeed more cases of severe flooding in those cases with high soil saturation. However, a different pattern is shown for the other two flood severity indices (duration and magnitude), where there is a higher conditional probability of severe flooding for lower (drier) antecedent soil moisture. Areas that are drier climatologically (e.g., the Arabian Peninsula) show higher return periods being exceeded, which is likely due to a combination of flash flooding, and the difficulty of accurately estimating return period thresholds in arid areas. Using soil moisture anomaly data rather than soil moisture saturation in future studies may help to further unpack this complex relationship.

e. Interplay of characteristics in modulating flood severity

The interplay between different characteristics acts to modulate the overall flood severity. For example, although fast-moving storms can mitigate fluvial flooding, there can still be a significant flood event if there are other risk factors present. An example of this is Typhoon Hagibis, which led to widespread and severe flooding in Japan in 2019. Here, the relative mitigation of Hagibis being fast moving was outweighed by the storm's size, intensity, and wider atmospheric environment, leading to very heavy precipitation and severe flooding, albeit over a relatively short period (Takemi and Unuma 2020). Contrastingly, although slow-moving storms significantly increase the conditional probability of a severe flood event, many slow-moving storms do not lead to significant flooding e.g., Tropical Storm Beryl (2012), which moved very slowly over northern Florida, but was relatively small and weak, and passed over an area where the antecedent conditions were dry. As this study included over 250 cases it was not possible to explore in detail the varied complexities that contributed to the detailed flood response in each individual case, such as the wider atmospheric environment, in a way that would be possible if only examining one or two cases. Nevertheless it provides a systematic analysis of potential meteorological and hydrological drivers, and a key finding is that the more driving factors a case possesses, the higher the likelihood of severe flooding, with in particular TCs that were slow, large, and strong, with wet antecedent conditions, having a higher flood severity in terms of the area that was affected.

f. Implications for research into the predictability of fluvial flooding from TCs

The severity of flooding in TC cases is shown to be dependent on a range of both meteorological and hydrological factors, showing the importance of a multidisciplinary Earth system approach to global flood prediction (Harrigan et al. 2020c). The flood forecasts from hydrometeorological forecasting systems will be highly dependent on how reliably the

input meteorological forecasts are able to predict not only the track and the intensity of TCs, but also their precipitation extent and intensity. This in turn will be dependent on the size and in particular the translation speed of the storm. There has generally been less focus on verifying these characteristics of TCs in ensemble forecasts, with most studies focusing on the predictability of track, intensity, and genesis. To understand and improve the forecasts of fluvial flooding from TCs, studies evaluating these aspects of forecast performance are recommended. It would also be beneficial to examine how uncertainty in each aspect of the forecast, and in each part of the forecasting chain, impacts on the overall predictability of fluvial flooding for TCs.

g. Implications for disaster risk reduction, preparedness, and response

The finding that the forward speed of the storm is of more importance than the intensity in modulating the severity of fluvial flooding is an important result. The expected speed of movement of the storm tends to have far less coverage in both traditional and social media than the intensity of the storm. This means that the public, local emergency responders, and those involved in planning disaster risk reduction activities may become too focused on storm intensity categories when making evacuation decisions, undertaking storm preparedness activities, or planning deployment of resources. Significant impacts from fluvial flooding can occur regardless of whether it is a strong storm, where there will likely also be significant wind and storm surge hazards, or a weak storm, where the fluvial flooding may be the main hazard. Both circumstances have important implications for forecast-based early action. An example of a TC that caused significant flooding while being relatively weak is Cyclone Komen, which impacted Myanmar, Bangladesh and India in 2015. Komen only reached equivalent strength of a tropical storm, but was very slow moving, with a broad circulation leading to prolonged heavy rainfall over areas of Myanmar already saturated due to weeks of monsoonal flooding, leading to severe impacts. Raising the profile of cases such as these where the wind hazards may be relatively low, but there is potential for a slow-moving storm impacting vulnerable areas, meaning the fluvial flood hazard and impacts are likely to be more severe, will help to ensure that preparations are made to ameliorate impact. For intense TCs, where evacuations and deployment of aid may be being organized in advance of landfall due to the anticipated wind impacts, it is also vital to know whether that storm also has an elevated likelihood of fluvial flooding due to other risk factors such as a slow translation speed or saturated antecedent soil conditions. If it does it would be important to select evacuation routes, shelters and aid deployment sites that would not be impacted in the event of extensive fluvial flooding, which may extend far from the landfall location. For example, Cyclone Idai, which led to catastrophic flooding in Mozambique in March 2019, exhibited most of the factors shown in this study to be key drivers of fluvial flood hazard: it was a strong storm, but significantly it was also a slow-moving storm at and after landfall, a relatively large storm, and also had wet antecedent soil moisture conditions. Highlighting this co-occurrence of flood drivers to decision-makers in future cases in which a storm is approaching landfall will help to ensure early action can be taken to plan for and mitigate the impacts of severe flooding.

6. Conclusions

Landfalling TCs over the last decade have been classified in terms of the severity of fluvial flooding that was associated with each storm using GloFAS-ERA5 reanalyses. Flood severity has been calculated using three different indices, each focusing on a different characteristic of the associated fluvial flooding (area, duration and magnitude). The key factors that impact the severity of fluvial flooding were investigated by comparing these flood severities with a range of TC characteristics (storm speed, size, shape, intensity, and precipitation), and catchment characteristics (antecedent soil moisture, orography, and gradient). The key findings are the following.

- There are cases that have very high flood severity in one measure and not in another, highlighting the importance of considering the area, duration and magnitude characteristics of TC flood events.
- Flood severity is strongly positively correlated with metrics summarizing the event total precipitation, showing the importance of increasing the availability and profile of precipitation forecasts in TC forecast communication and verifying the ability of models that drive flood forecasting systems to forecast the precipitation associated with TCs.
- Slow-moving storms were found to have a much higher conditional probability of a severe flood event relative to fast-moving storms, confirming that slower-moving storms, where storms are raining over an area for longer, tend to have higher flood severity.
- All intensities of TC have cases spanning the full range of flood severity values, including several cases of tropical storm strength that were associated with severe flooding. This confirms the need for forecasting agencies to continue emphasizing that the fluvial flood hazard can be severe in all categories of TC.
- Large storms have a higher conditional probability of severe flooding than small storms in terms of the area affected. The duration and magnitude of the flooding are found to be more dependent on the catchment characteristics within the land footprint of the storm, with gentler slopes having a much greater conditional probability of severe flooding. The relationship between flood severity and antecedent soil moisture is found to be complex and not consistent across the different flood severity indices.
- Several TC and catchment characteristics often combine to influence the overall flood severity and negate or enhance other factors e.g., fast-moving storms still having a severe flood hazard if they are large, intense and passing over saturated ground. The more driving factors that a case possesses the higher the flood risk is found to be, with the highest likelihood of having a large area affected by flooding found for TCs that were slow, large, intense, and affecting areas with wet antecedent conditions.

The reanalysis data used in this study provide a proxy for the observed severity of flooding, and, although this allows a direct

comparison of flood severity across all TC cases, studies of fluvial flooding in TCs would benefit hugely from an increase in the availability and consistency of hydrological observations (Lavers et al. 2019).

This study has highlighted the characteristics of TCs that have the most control on flood hazard. For those involved in communicating early warnings and taking forecast-based action before a storm our results show the importance of considering aspects such as storm speed when assessing the risks. For developers of hydrometeorological ensemble forecasts of river flows our work underlines that the input meteorological ensemble forecasts for TCs need to be able to reliably predict not just their track and intensity, but also their precipitation, size and translation speed. Future research needs to focus on verifying and improving these characteristics for agencies to be able to provide more accurate forecasts of flood hazard.

Acknowledgments. The authors thank three anonymous reviewers for their helpful comments and suggestions, which led to improvements to the paper. Authors Helen Titley and Joanne Robbins acknowledge the support of the Weather and Climate Science for Service Partnership (WCSSP) India and South East Asia projects, supported by the U.K. government's Newton Fund. Authors Liz Stephens and Hannah Cloke acknowledge funding from the U.K.'s Natural Environment Research Council (NERC) and Foreign Commonwealth & Development Office (FCDO) (formerly DFID) Science for Humanitarian Emergencies and Resilience (SHEAR) research program Forecasts for Anticipatory Humanitarian Action (FATHUM) project Grant NE/P000525/1. Author Hannah Cloke also acknowledges funding from the U.K.'s Natural Environment Research Council (NERC) The Evolution of Global Flood Risk (EVOFLOOD) project Grant NE/S015590/1.

Data availability statement. The data used in this study were accessed from the following freely available sources: (i) GPM IMERG final data (https://doi.org/10.5067/GPM/IMERG/3B-HH/06), (ii) ERA5 (precipitation, MSLP, and soil moisture) (https://doi.org/10.24381/cds.adbb2d47), (iii) GloFAS-ERA5 (https://doi.org/10.24381/cds.a4fdd6b9), and (iv) IBTrACS (https://doi.org/10.25921/82ty-9e16).

REFERENCES

Alfieri, L., P. Burek, E. Dutra, B. Krzeminski, D. Muraro, J. Thielen, and F. Pappenberger, 2013: GloFAS—Global ensemble streamflow forecasting and flood early warning. *Hydrol. Earth Syst. Sci.*, **17**, 1161–1175, https://doi.org/10.5194/hess-17-1161-2013.

——, E. Zsoter, S. Harrigan, F. Aga Hirpa, C. Lavaysse, C. Prudhomme, and P. Salamon, 2019: Range-dependent thresholds for global flood early warning. *J. Hydrol. X*, **4**, 100034, https://doi.org/10.1016/j.hydroa.2019.100034.

Associated Press, 2018: Yemen says 14 killed in Cyclone Luban. Accessed 15 September 2020, https://apnews.com/705065c5517545adae9e4fb313bb8381.

Balsamo, G., A. Beljaars, K. Scipal, P. Viterbo, B. van den Hurk, M. Hirschi, and A. K. Betts, 2009: A revised hydrology for the ECMWF model: Verification from field site to terrestrial water storage and impact in the Integrated Forecast System. *J. Hydrometeor.*, **10**, 623–643, https://doi.org/10.1175/2008JHM1068.1.

——, F. Pappenberger, E. Dutra, P. Viterbo, and B. van den Hurk, 2011: A revised land hydrology in the ECMWF model: A step towards daily water flux prediction in a fully-closed water cycle. *Hydrol. Processes*, **25**, 1046–1054, https://doi.org/10.1002/hyp.7808.

Beck, H. E., and Coauthors, 2019: Daily evaluation of 26 precipitation datasets using Stage-IV gauge-radar data for the CONUS. *Hydrol. Earth Syst. Sci.*, **23**, 207–224, https://doi.org/10.5194/hess-23-207-2019.

Berghuijs, W. R., S. Harrigan, P. Molnar, L. J. Slater, and J. W. Kirchner, 2019: The relative importance of different flood-generating mechanisms across Europe. *Water Resour. Res.*, **55**, 4582–4593, https://doi.org/10.1029/2019WR024841.

Chen, S. S., J. A. Knaff, and F. D. Marks, 2006: Effects of vertical wind shear and storm motion on tropical cyclone rainfall asymmetries deduced from TRMM. *Mon. Wea. Rev.*, **134**, 3190–3208, https://doi.org/10.1175/MWR3245.1.

Cheung, K., and Coauthors, 2018: Recent advances in research and forecasting of tropical cyclone rainfall. *Trop. Cyclone Res. Rev.*, **7**, 106–127, https://doi.org/10.6057/2018TCRR02.03.

Coughlan de Perez, E., and Coauthors, 2016: Action-based flood forecasting for triggering humanitarian action. *Hydrol. Earth Syst. Sci.*, **20**, 3549–3560, https://doi.org/10.5194/hess-20-3549-2016.

Czajkowski, J., and E. Kennedy, 2010: Fatal tradeoff? Toward a better understanding of the costs of not evacuating from a hurricane in landfall counties. *Popul. Environ.*, **31**, 121–149, https://doi.org/10.1007/s11111-009-0097-x.

——, G. Villarini, M. Montgomery, E. Michel-Kerjan, and R. Goska, 2017: Assessing current and future freshwater flood risk from North Atlantic tropical cyclones via insurance claims. *Sci. Rep.*, **7**, 41609, https://doi.org/10.1038/srep41609.

ECMWF, 2020: IFS documentation CY47R1—Part IV: Physical processes. ECMWF Rep., 228 pp., https://doi.org/10.21957/cpmkqvhja.

Emerton, R., and Coauthors, 2020: Emergency flood bulletins for Cyclones Idai and Kenneth: A critical evaluation of the use of global flood forecasts for international humanitarian preparedness and response. *Int. J. Disaster Risk Reduct.*, **50**, 101811, https://doi.org/10.1016/j.ijdrr.2020.101811.

Ficchì, A., and L. Stephens, 2019: Climate variability alters flood timing across Africa. *Geophys. Res. Lett.*, **46**, 8809–8819, https://doi.org/10.1029/2019GL081988.

Guo, L., N. P. Klingaman, P. L. Vidale, A. G. Turner, M. Demory, and A. Cobb, 2017: Contribution of tropical cyclones to atmospheric moisture transport and rainfall over East Asia. *J. Climate*, **30**, 3853–3865, https://doi.org/10.1175/JCLI-D-16-0308.1.

Harrigan, S., E. Zsoter, C. Barnard, F. Wetterhall, P. Salamon, and C. Prudhomme, 2019: River discharge and related historical data from the Global Flood Awareness System, v2.1. Copernicus Climate Change Service (C3S) Climate Data Store (CDS), accessed 8 October 2020, https://doi.org/10.24381/cds.a4fdd6b9.

——, ——, H. Cloke, P. Salamon, and C. Prudhomme, 2020a: Daily ensemble river discharge reforecasts and real-time forecasts from the operational Global Flood Awareness System. *Hydrol. Earth Syst. Sci. Discuss.*, https://doi.org/10.5194/hess-2020-532.

——, and Coauthors, 2020b: GloFAS-ERA5 operational global river discharge reanalysis 1979–present. *Earth Syst. Sci. Data*, **12**, 2043–2060, https://doi.org/10.5194/essd-12-2043-2020.

——, H. Cloke, and F. Pappenberger, 2020c: Innovating global hydrological prediction through an Earth system approach. *WMO Bull.*, **69**, https://public.wmo.int/en/resources/bulletin/innovating-global-hydrological-prediction-through-earth-system-approach.

Heming, J. T., 2017: Tropical cyclone tracking and verification techniques for Met Office numerical weather prediction models. *Meteor. Appl.*, **24**, 1–8, https://doi.org/10.1002/met.1599.

Hernández Ayala, J. J., and C. J. Matyas, 2016: Tropical cyclone rainfall over Puerto Rico and its relations to environmental and storm-specific factors. *Int. J. Climatol.*, **36**, 2223–2237, https://doi.org/10.1002/joc.4490.

Hersbach, H., and Coauthors, 2018a: ERA5 hourly data on single levels from 1979 to present. Copernicus Climate Change Service (C3S) Climate Data Store (CDS), accessed 8 October 2020, https://doi.org/10.24381/cds.adbb2d47.

——, and Coauthors, 2018b: Operational global reanalysis: Progress, future directions and synergies with NWP. ECMWF ERA Rep. Series 27, 63 pp., https://doi.org/10.21957/tkic6g3wm.

——, and Coauthors, 2020: The ERA5 global reanalysis. *Quart. J. Roy. Meteor. Soc.*, **146**, 1999–2049, https://doi.org/10.1002/qj.3803.

Hirpa, F. A., P. Salamon, H. E. Beck, V. Lorini, L. Alfieri, E. Zsoter, and S. J. Dadson, 2018: Calibration of the Global Flood Awareness System (GloFAS) using daily streamflow data. *J. Hydrol.*, **566**, 595–606, https://doi.org/10.1016/j.jhydrol.2018.09.052.

Huffman, G. J., E. F. Stocker, D. T. Bolvin, E. J. Nelkin, and T. Jackson, 2019: GPM IMERG Final Precipitation L3 Half Hourly 0.1 degree × 0.1 degree V06. Goddard Earth Sciences Data and Information Services Center (GES DISC), accessed 6 July 2020, https://doi.org/10.5067/GPM/IMERG/3B-HH/06.

Jiang, H., C. Liu, and E. J. Zipser, 2011: A TRMM-based tropical cyclone cloud and precipitation feature database. *J. Appl. Meteor. Climatol.*, **50**, 1255–1274, https://doi.org/10.1175/2011JAMC2662.1.

Jiang, Q., and Coauthors, 2021: Evaluation of the ERA5 reanalysis precipitation dataset over Chinese Mainland. *J. Hydrol.*, **595**, 125660, https://doi.org/10.1016/j.jhydrol.2020.125660.

Khouakhi, A., G. Villarini, and G. A. Vecchi, 2017: Contribution of tropical cyclones to rainfall at the global scale. *J. Climate*, **30**, 359–372, https://doi.org/10.1175/JCLI-D-16-0298.1.

Knapp, K. R., M. C. Kruk, D. H. Levinson, H. J. Diamond, and C. J. Neumann, 2010: The International Best Track Archive for Climate Stewardship (IBTrACS): Unifying tropical cyclone best track data. *Bull. Amer. Meteor. Soc.*, **91**, 363–376, https://doi.org/10.1175/2009BAMS2755.1.

——, H. J. Diamond, J. P. Kossin, M. C. Kruk, and C. J. Schreck III, 2018: International Best Track Archive for Climate Stewardship (IBTrACS) Project, version 4 (subset: since 1980). NOAA/National Centers for Environmental Information, accessed 28 September 2020, https://doi.org/10.25921/82ty-9e16.

Knutson, T. R., and Coauthors, 2010: Tropical cyclones and climate change. *Nat. Geosci.*, **3**, 157–163, https://doi.org/10.1038/ngeo779.

Kossin, J. P., 2018: A global slowdown of tropical-cyclone translation speed. *Nature*, **558**, 104–107, https://doi.org/10.1038/s41586-018-0158-3.

Lavers, D., S. Harrigan, E. Andersson, D. S. Richardson, C. Prudhomme, and F. Pappenberger, 2019: A vision for improving global flood forecasting. *Environ. Res. Lett.*, **14**, 121002, https://doi.org/10.1088/1748-9326/ab52b2.

Luitel, B., G. Villarini, and G. A. Vecchi, 2018: Verification of the skill of numerical weather prediction models in forecasting rainfall from U.S. landfalling tropical cyclones. *J. Hydrol.*, **556**, 1026–1037, https://doi.org/10.1016/j.jhydrol.2016.09.019.

Merrill, R. T., 1984: A comparison of large and small tropical cyclones. *Mon. Wea. Rev.*, **112**, 1408–1418, https://doi.org/10.1175/1520-0493(1984)112<1408:ACOLAS>2.0.CO;2.

Nogueira, M., 2020: Inter-comparison of ERA-5, ERA-Interim and GPCP rainfall over the last 40 years: Process-based analysis of systematic and random differences. *J. Hydrol.*, **583**, 124632, https://doi.org/10.1016/j.jhydrol.2020.124632.

Prat, O. P., and B. R. Nelson, 2013: Mapping the world's tropical cyclone rainfall contribution over land using the TRMM Multi-satellite Precipitation Analysis. *Water Resour. Res.*, **49**, 7236–7254, https://doi.org/10.1002/wrcr.20527.

——, and ——, 2016: On the link between tropical cyclones and daily rainfall extremes derived from global satellite observations. *J. Climate*, **29**, 6127–6135, https://doi.org/10.1175/JCLI-D-16-0289.1.

Qiu, W., F. Ren, L. Wu, L. Chen, and C. Ding, 2019: Characteristics of tropical cyclone extreme precipitation and its preliminary causes in Southeast China. *Meteor. Atmos. Phys.*, **131**, 613–626, https://doi.org/10.1007/s00703-018-0594-5.

Rappaport, E. N., 2000: Loss of life in the United States associated with recent Atlantic tropical cyclones. *Bull. Amer. Meteor. Soc.*, **81**, 2065–2074, https://doi.org/10.1175/1520-0477(2000)081<2065:LOLITU>2.3.CO;2.

——, 2014: Fatalities in the United States from Atlantic tropical cyclones: New data and interpretation. *Bull. Amer. Meteor. Soc.*, **95**, 341–346, https://doi.org/10.1175/BAMS-D-12-00074.1.

Rezapour, M., and T. E. Baldock, 2014: Classification of hurricane hazards: The importance of rainfall. *Wea. Forecasting*, **29**, 1319–1331, https://doi.org/10.1175/WAF-D-14-00014.1.

Rogers, R., F. Marks, and T. Marchok, 2009: Tropical cyclone rainfall. *Encyclopedia of Hydrological Sciences*, M. G. Anderson and J. J. McDonnell, Eds., John Wiley and Sons, https://doi.org/10.1002/0470848944.hsa030.

Saha, K. K., M. M. Hasan, and A. Quazi, 2015: Forecasting tropical cyclone-induced rainfall in coastal Australia: Implications for effective flood management. *Austral. J. Environ. Manage.*, **22**, 446–457, https://doi.org/10.1080/14486563.2015.1028109.

Shi, C., J. Wu, and L. Qi, 2017: Analysis on precipitation difference of two typhoons with similar tracks. *J. Mar. Meteor.*, **37**, 36–45.

Song, J. Y., A. Alipour, H. Moftakhari, and H. Moradkhani, 2020: Toward a more effective hurricane hazard communication. *Environ. Res. Lett.*, **15**, 064012, https://doi.org/10.1088/1748-9326/ab875f.

Stein, R. M., L. Dueñas-Osorio, and D. Subramanian, 2010: Who evacuates when hurricanes approach? The role of risk, information, and location. *Soc. Sci. Quart.*, **91**, 816–834, https://doi.org/10.1111/j.1540-6237.2010.00721.x.

Stephens, E., J. J. Day, F. Pappenberger, and H. Cloke, 2015: Precipitation and floodiness. *Geophys. Res. Lett.*, **42**, 10 316–10 323, https://doi.org/10.1002/2015GL066779.

Sturdevant-Rees, P., J. A. Smith, J. Morrison, and M. L. Baeck, 2001: Tropical storms and the flood hydrology of the central Appalachians. *Water Resour. Res.*, **37**, 2143–2168, https://doi.org/10.1029/2000WR900310.

Takemi, T., and T. Unuma, 2020: Environmental factors for the development of heavy rainfall in the eastern part of Japan during Typhoon Hagibis (2019). *SOLA*, **16**, 30–36, https://doi.org/10.2151/sola.2020-006.

Tarek, M., F. P. Brissette, and R. Arsenault, 2020: Evaluation of the ERA5 reanalysis as a potential reference dataset for hydrological modelling over North America. *Hydrol. Earth Syst. Sci.*, **24**, 2527–2544, https://doi.org/10.5194/hess-24-2527-2020.

Titley, H. A., R. L. Bowyer, and H. L. Cloke, 2020: A global evaluation of multi-model ensemble tropical cyclone track probability forecasts. *Quart. J. Roy. Meteor. Soc.*, **146**, 531–545, https://doi.org/10.1002/qj.3712.

Touma, D., S. Stevenson, S. J. Camargo, D. E. Horton, and N. S. Diffenbaugh, 2019: Variations in the intensity and spatial extent of tropical cyclone precipitation. *Geophys. Res. Lett.*, **46**, 13 992–14 002, https://doi.org/10.1029/2019GL083452.

Towner, J., A. Ficchí, H. L. Cloke, J. Bazo, E. Coughlan de Perez, and E. M. Stephens, 2020: Influence of ENSO and tropical Atlantic climate variability on flood characteristics in the Amazon basin. *Hydrol. Earth Syst. Sci. Discuss.*, https://doi.org/10.5194/hess-2020-580.

Van Der Knijff, J. M., J. Younis, and A. P. J. De Roo, 2010: LISFLOOD: A GIS-based distributed model for river basin scale water balance and flood simulation. *Int. J. Geogr. Info. Sci.*, **24**, 189–212, https://doi.org/10.1080/13658810802549154.

Villarini, G., R. Goska, J. A. Smith, and G. A. Vecchi, 2014: North Atlantic tropical cyclones and U.S. flooding. *Bull. Amer. Meteor. Soc.*, **95**, 1381–1388, https://doi.org/10.1175/BAMS-D-13-00060.1.

Weber, H. C., C. F. Lok, N. E. Davidson, and Y. Xiao, 2014: Objective estimation of the radius of the outermost closed isobar in tropical cyclones. *Trop. Cyclone Res. Rev.*, **3**, 1–21, https://doi.org/10.6057/2014TCRR01.01.

Whitehead, J. C., R. Edwards, M. Van Willigen, J. R. Maiolo, K. Wilson, and K. T. Smith, 2000: Heading for higher ground: Factors affecting real and hypothetical hurricane evacuation behavior. *Global Environ. Change*, **2B**, 133–142, https://doi.org/10.1016/S1464-2867(01)00013-4.

Yu, Z., Y. Wang, H. Xu, N. Davidson, Y. Chen, Y. Chen, and H. Yu, 2017: On the relationship between intensity and rainfall distribution in tropical cyclones making landfall over China. *J. Appl. Meteor. Climatol.*, **56**, 2883–2901, https://doi.org/10.1175/JAMC-D-16-0334.1.

Yuan, S., L. Zhu, and S. M. Quiring, 2021: Comparison of two multisatellite algorithms for estimation of tropical cyclone precipitation in the United States and Mexico: TMPA and IMERG. *J. Hydrometeor.*, **22**, 923–939, https://doi.org/10.1175/JHM-D-19-0296.1.

Zhou, Y., and C. J. Matyas, 2017: Spatial characteristics of storm-total rainfall swaths associated with tropical cyclones over the eastern United States. *Int. J. Climatol.*, **37**, 557–569, https://doi.org/10.1002/joc.5021.

Zsótér, E., H. L. Cloke, C. Prudhomme, S. Harrigan, P. de Rosnay, J. Muñoz-Sabater, and E. Stephens, 2020: Trends in the GloFAS-ERA5 river discharge reanalysis. ECMWF Tech. Memo. 871, 73 pp., https://www.ecmwf.int/sites/default/files/elibrary/2020/19762-trends-glofas-era5-river-discharge-reanalysis.pdf.